ACS Catalysis

Letter

pubs.acs.org/acscatalysis

Quantitative Analysis of Bioactive NAD$^+$ Regenerated by NADH Electro-oxidation

Hanzi Li, Kathryn E Worley, and Scott Calabrese Barton*

Department of Chemical Engineering and Materials Science, Michigan State University, East Lansing, Michigan 48824, United States

Supporting Information

ABSTRACT: The bioactivity of NAD$^+$ electrogenerated at a high-surface-area composite anode was verified spectroscopically. The anode was composed of poly(methylene green) electropolymerized on carbon nanotubes (PMG-CNT) which was in turn immobilized on carbon paper. A mathematical model calibrated by measurements of NADH oxidation at PMG-CNT-modified glassy carbon electrodes was applied to predict transient NADH consumption. The model showed good agreement with the experimental data, and 80% conversion of NADH was observed after 1 h of electrochemical oxidation. Using a spectroscopic enzyme cycling assay, the yield of enzymatically active NAD$^+$ was verified at 93% and 87% for applied potentials of 500 and 150 mV vs Ag|AgCl, respectively. This suggests that roughly 10% of oxidized NADH may be lost due to dimerization or some other side reaction after accounting for self-decay. These results prove that bioactive NAD$^+$ can be efficiently produced using electrochemical techniques, enabling application in bioconversion, biosensor, and bioenergy processes.

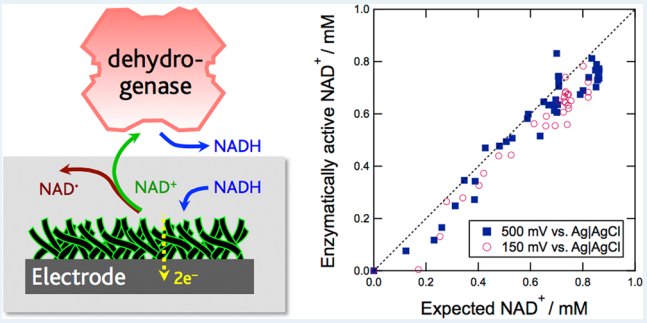

KEYWORDS: *NADH electrocatalysis, bioactive electro-generated NAD$^+$, quantitative yield, enzyme cycling assay*

INTRODUCTION

Nicotinamide adenine dinucleotide (NADH)-dependent dehydrogenases are promising bioelectrocatalysts because of their ubiquity and the low redox potential of the NADH/NAD$^+$ couple (0.09 V vs RHE).[1−13] For example, use of NADH-dependent enzymes for the production of a wide range of compounds such as dihydroxyacetone,[3] gluconic acid,[4] and cyclohexanone[5] has been reported. Dehydrogenase biosensors have been studied for detecting lactate,[6] glucose,[7] and isocitrate[13] in the Kreb's cycle. Fuel cells based on oxidation of alcohol,[9−11] glucose[14] and malate[12] by NADH-dependent dehydrogenase have been investigated, as well.

Electrochemical recycling of NAD$^+$ is essential to dehydrogenase-based bioconversion, biosensor, and bioenergy processes; however, the direct electrogeneration of NAD$^+$ is slow at conventional electrodes and requires high overpotential.[1,2,15,16] Numerous strategies have been evaluated for electrochemical regeneration of NAD$^+$. Electrocatalysts such as poly(azines),[2,17,18] poly(aniline),[19] metal oxides,[20,21] and the enzyme diaphorase[9,15] have been reported. Porous or high-surface-area materials such as reticulated vitreous carbon (RVC),[22−25] carbon nanotubes (CNT),[26−31] and graphene-modified graphite[32] have been employed to increase the surface area of NADH-oxidizing electrodes. For example, Villarrubia et al. have electropolymerized methylene green (MG) on CNT-based "bucky papers" and observed electrocatalytic activity toward NADH oxidation and L-malate oxidation.[31]

Although many materials have been demonstrated to possess activity for NADH electrocatalysis, there are few reports verifying the bioactivity of electrogenerated NAD$^+$ by NADH oxidation, especially for high-rate electrodes.[10,16,22−25,31,33−37] As suggested by Elving et al.,[38,39] Chi et al.,[40] and Gorton et al.,[16,41] the first step of NADH electrocatalysis is deprotonation to NADH$^{\bullet+}$, which leads to the conversion of NADH to NAD$^\bullet$ radicals after releasing one proton. The NAD$^\bullet$ radicals may subsequently dimerize to NAD_2 or react with the solvent medium, resulting in nonbioactive products.[38] Similarly, Karyakin et al. have reported that nonbioactive 1,6-NADH is generated as a byproduct in NAD$^+$ electroreduction.[42] Thus, it is crucial to verify enzymatic activity of the products of NADH electrooxidation.

In the late 1970s, Kelly et al. demonstrated enzymatically active NAD$^+$ that was generated on a carbon electrode using alcohol dehydrogenase,[37] but their optimal applied potential was as high as 1.2 V vs RHE, and at least 6 h was required to achieve more than 80% NADH conversion.[37] Laval et al.,[23,24] Bonnefoy et al.,[22] and Fassouana et al.[25] used RVC electrodes and reported turnover numbers above 3000 s^{-1}. Nevertheless, a similarly high applied potential was needed.[22−25] To reduce this overpotential, Tse et al., for the first time, utilized chemically modified electrodes for NADH electrocatalysis and confirmed

Received: July 10, 2012
Revised: October 3, 2012
Published: October 18, 2012

that the product was enzymatically active NAD^+,[33] but the current was observed only in the microampere range, indicating a low kinetic rate.[33]

Recently, researchers have explored and characterized advanced materials for NADH electrocatalysis. Zhang et al. fabricated graphene oxide and reduced graphene oxide-modified screen-printed electrodes to oxidize NADH[34] and observed NADH oxidation by monitoring the absorbance at 260 and 340 nm in spectroscopy,[34] but they did not verify the enzymatic activity of the electrogenerated NAD^+.[34]

Because of the good stability and the ability to reduce overpotential, electrodes modified by electropolymerized azines have been employed in biosensor and bioenergy applications;[31,35,36] however, NAD^+ was generally introduced as a reactant when characterizing such electrodes, preventing observation of bioactivity in purely electroregenerated NAD^+.[31,35,36] Alpat et al. developed an alcohol dehydrogenase biosensor based on NADH electrocatalysis by toluidine blue O,[10] and their report indirectly confirmed that the generated NAD^+ was enzymatically active, since their system did not contain NAD^+ in the initial operation conditions.[10] However, the quantitative efficiency of NADH electrocatalysis, which we define as the percentage yield of enzymatically active NAD^+ produced by electro-oxidation of NADH, has remained unclear.[10]

In our previous work, we fabricated high-rate NADH-oxidizing electrodes by electropolymerizing azines on CNT-modified GC electrodes, and a mathematical model was developed for quantitative analysis.[43,44] We tested several electrocatalysts, including carbon nanotubes (CNT-GC), poly(toluidine blue O) (PTBO-GC), and poly(methylene green) (PMG-GC), for activity toward NADH electrooxidation and found that the incorporation of PMG and CNT (PMG-CNT-GC) leads to the highest NADH oxidation rate.[43] In this study, we immobilize PMG-CNT on a carbon paper support to construct a high-surface-area electrode for bulk conversion of NADH to NAD^+. Capacitance measurements on CNT−carbon paper indicate electrochemical properties similar to CNT-GC, including a controllable high surface area and good reproducibility. Bulk NADH oxidation was performed on PMG-CNT−carbon paper, with conversion monitored using spectroscopic absorbance at 340 nm. The process was simulated using a kinetic model calibrated with data from rotating disk electrode experiments. Using this enzyme cycling assay, we quantitatively verified the yield of enzymatically active NAD^+ on PMG-modified high-surface-area electrodes.

EXPERIMENTAL SECTION

Chemicals and Materials. NADH, methylene green (MG), sodium tetraborate, and sodium nitrate were purchased from Sigma-Aldrich (St. Louis, MO). Sodium phosphate monobasic and sodium phosphate diabasic were obtained from J.T. Baker (Phillipsburg, NJ). *N,N*-dimethylformamide (DMF) was obtained from Fisher BioReagents (Hampton, NH). All materials were used as received without further purification. Buffer solutions were prepared with deionized water. Ultrapure argon gas was purchased from Airgas (Lansing, MI). Carboxylated multiwalled carbon nanotubes (9.5 nm diameter, 1.5 μm length, > 95% purity), were obtained from Nanocyl (NC3101, Sambreville, Belgium). Carbon paper was obtained from ElectroChem (EC TP1 030, Woburn, MA).

CNT Deposition on Carbon Electrode. CNT modification of carbon electrodes was reported previously.[43,45] Essentially, 2 mg mL^{-1} CNT ink was dispersed ultrasonically in DMF solvent. The CNT-modified carbon electrode (CNT-CP) was fabricated by air-brushing CNT ink on carbon paper (CP) and vacuum-drying.

Electropolymerization of Methylene Green. As previously reported,[2,43] deposition of poly methylene green on CNT-CP was achieved via electropolymerization using cyclic voltammetry (CV) with a scan rate of 50 mV s^{-1} between −0.5 and 1.5 V vs Ag|AgCl (4 M KCl) for 20 cycles in fresh MG solution. MG solution was prepared by dissolving 0.4 mM MG in 0.01 M borate buffer, pH 9.1, with 0.1 M $NaNO_3$. The resulting MG solution was purged with argon for 20 min to eliminate oxygen. During electropolymerization, argon was continuously bubbled to maintain an oxygen-free solution.

Capacitance Characterization. Capacitive surface area was estimated using CV in the narrow potential range from 0.3 to 0.4 V vs Ag|AgCl (4 M KCl) with varying scan rates from 50 to 100 mV s^{-1} in supporting electrolyte (0.01 M borate buffer pH 9.1, 0.1 M $NaNO_3$, 30 °C). This electrolyte was chosen because it serves as a buffer solution for electropolymerization. Plotting the current in the nonfaradic potential region against scan rate, the slope was recorded as capacitance. Assuming a specific capacitance of 25 μF cm^{-2} for carbon material,[46] the electrode surface area was thus evaluated. Prior to electropolymerization of PMG on CNT-CP, capacitance was measured to ensure consistent values for all CNT-CP electrodes.

NADH Bulk Oxidation. NADH oxidation was performed using PMG-CNT-CP as the working electrode, with an initial NADH concentration of 0.94 mM in 20 mL pH 6 phosphate buffer at 30 °C, constant applied potential of 0.15 or 0.5 V vs Ag|AgCl (4 M KCl), and magnetically stirred with a 10 mm × 3 mm stirring bar at 1200 rpm. The exposed electrode surface area was 0.8 cm^2. The electrolyte was purged with argon to exclude oxygen.

During reaction, the NADH concentration was monitored at 10 min intervals by analyzing 160 μL samples of the reactor solution at 5-fold dilution by absorbance spectroscopy at 340 nm with an extinction coefficient of ε = 6220 M^{-1} cm^{-1}. To quantify the enzymatic activity of electrogenerated NAD^+, a commercially available enzyme cycling assay (EnzyChrom *NAD^+/NADH Assay Kit*, ECND-100) was employed to analyze the bulk solution during and after electrocatalysis. The scheme for the cycling assay is shown in Figure 1. The working reagents

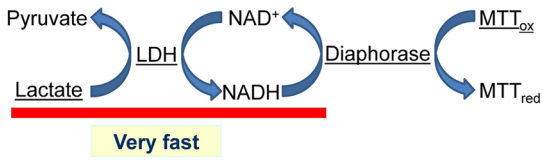

Figure 1. Scheme of EnzyChrom enzyme cycling assay.

of the assay include lactate, lactate dehydrogenase (LDH), diaphorase and formazan (MTT_{ox}), which are underlined in Figure 1. The assay kit relies on the excess activity of LDH to fully reduce all NAD^+ present to NADH, which in turn reduces the MTT_{ox} reagent via the NADH-oxidizing enzyme diaphorase. After a 15 min reaction time, the absorbance of reduced MTT_{red} measured at 565 nm is proportional to the combined concentration of NAD^+ and NADH, C_{NADtot}.[47−49] The concentration of NADH, C_{NADH}, was obtained by absorbance in the absence of the kit. The concentration of

dx.doi.org/10.1021/cs3004598 | ACS Catal. 2012, 2, 2572−2576

enzyme-active NAD^+ could then be calculated by subtraction: $C_{NAD+,\ active}(t) = C_{NADtot}(t) - C_{NADH}(t)$.

ANALYSIS

NADH electro-oxidation occurs according to the reaction

$$NADH \rightarrow NAD^+ + H^+ + 2e^- \quad (1)$$

NADH is consumed in a bulk electrolysis reactor as a result of the above reaction as well as bulk decay.[50−54] The consumption rate of NADH, R_{NADH} (mM min^{-1}), can therefore be expressed as

$$\frac{dC_{NADH}}{dt} = -R_{NAD+} - R_{decay} \quad (2)$$

where R_{NAD+} is the rate of NAD^+ generation according to eq 1, and is related to electrode current density, j, by

$$R_{NAD+} = \frac{j(t)\,A}{nFV} \quad (3)$$

where A is the geometric surface area of the electrode (0.8 cm^{-2}), V is the reactor volume (initially 20 mL, varying with time as 160 μL samples are withdrawn), n is the electron stoichiometric coefficient (2 equiv mol^{-1}), and F is Faraday's constant (96 485 C $equiv^{-1}$).

Based on previous work, current density j can be written as[43,44]

$$j(t) = j_{max}\left(\frac{C_{NADH}(t)}{K_S + C_{NADH}(t)}\right)\left(\frac{\exp[(E-U)/b]}{1+\exp[(E-U)/b]}\right) \quad (4)$$

where j_{max} is the adsorption-controlled plateau current density, K_S is the Langmuir adsorption coefficient, U is the half-wave potential, b is the exponential coefficient, E is the applied potential; and C_{NADH} is the bulk concentration of NADH.

Ambient self-decay of NADH, R_{decay}, can be expressed as a first-order reaction.

$$\frac{dC_{decay}}{dt} = k_{decay} \times C_{NADH}(t) \quad (5)$$

Under the conditions considered in this work, the decay constant, k_{decay}, was found experimentally to be 3.6 ± 0.4 h^{-1}, which is consistent with literature values,[53,55] as shown in the Supporting Information. Other parameters are listed in the Supporting Information. Using an initial NADH concentration of 0.94 mM with no NAD^+ initially present, the conversion of NADH to NAD^+ was simulated using the above equations in MATLAB.

Experimentally, the NADH concentration was measured using spectroscopic absorbance at 340 nm. The expected NAD^+ concentration, $C_{NAD+}(t)$, was calculated using

$$C_{NAD+}(t) = C^0_{NADH} - C_{NADH}(t) - C_{decay}(t) \quad (6)$$

where C^0_{NADH} is the initial NADH concentration, $C_{NADH}(t)$ is the measured NADH concentration obtained by spectroscopic absorbance, and $C_{decay}(t)$ is the decayed NADH obtained by integration of eq 5.

The yield of enzymatically active NAD^+ is calculated by

$$\text{yield} = \frac{C_{NAD+,active}(t)}{C_{NAD+}(t)} \quad (7)$$

where $C_{NAD+,\ active}(t)$ is measured by the EnzyChrom assay and $C_{NAD+}(t)$ is obtained from eq 6.

RESULTS AND DISCUSSION

CNT-Coated Carbon Support. Figure 2 shows the capacitive surface area of CNT-coated carbon paper compared with CNT-coated glassy carbon (GC) as it varies with CNT loading. The two curves appear to be linear within experimental error, with similar slopes (890 ± 18 and 860 ± 11 cm^2 mg^{-1}, for CNT-GC and CNT-CP-GC, respectively). Therefore, immobilization of carbon paper does not impact the active surface area of the CNT layer, suggesting that the deposited CNT possesses the same properties when supported on carbon paper support as on a GC electrode. The larger experimental error on CNT-CP-GC compared with CNT-GC is likely a

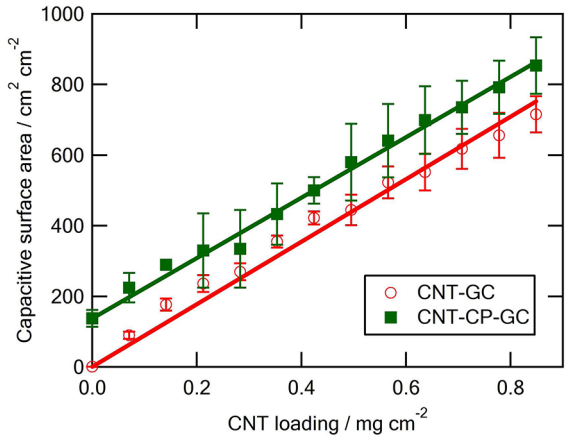

Figure 2. Capacitance of CNT-coated carbon paper (CNT-CP-GC) and CNT-coated glassy carbon (CNT-GC) for varying CNT loadings, obtained by cyclic voltammetry at varying scan rates in 0.01 M borate buffer pH 9.1, 0.1 M $NaNO_3$, 30 °C, potential range 0.3−0.4 V vs AgI AgCl.

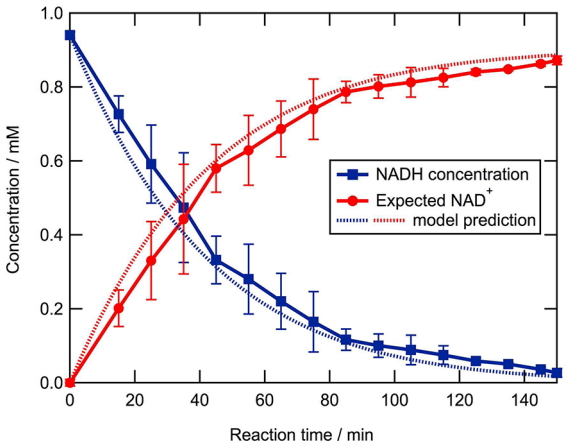

Figure 3. Electrochemical oxidation of NADH to NAD^+ in a batch reactor using a 0.8 cm^2 PMG-CNT-CP electrode. Markers and solid lines: experimental data. Dashed lines: simulation results. NADH oxidation was performed with NADH concentration initially at 0.94 mM in 20 mL pH 6, 30 °C phosphate buffer, applied potential of 0.5 V vs AgIAgCl, with 1200 rpm magnetic stirring. NADH concentration was measured by spectroscopic absorbance at 340 nm. Expected NAD^+ concentration was obtained by eq 6.

dx.doi.org/10.1021/cs3004598 | ACS Catal. 2012, 2, 2572−2576

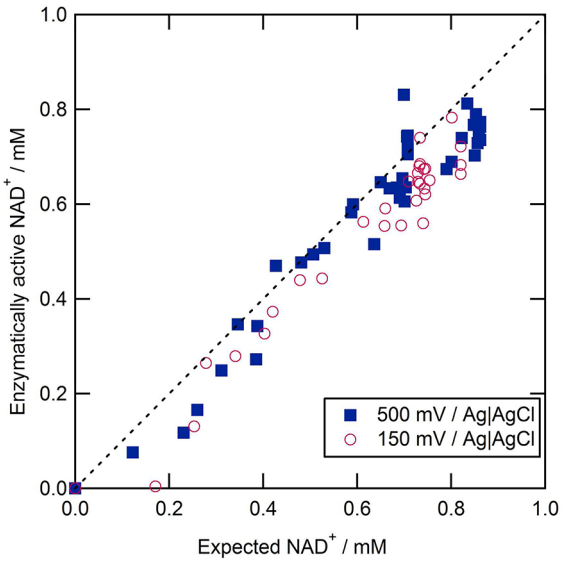

Figure 4. The yield of enzymatically active NAD^+ generated by NADH electrochemical oxidation. The concentration of active NAD^+ was measured using the enzyme cycling assay kit. The expected NAD^+ concentration was obtained by subtracting the measured NADH and decayed NADH from the initial concentration.

result of the increased complexity of assembling the electrode with the additional CP layer.

Conversions in NADH Bulk Oxidation on PMG-CNT-Carbon Paper. Poly(methylene green) (PMG) was deposited on CNT-CP via electropolymerization in borate buffer. For the current deposition conditions, the loading of PMG was previously found to be 560 nmol cm^{-2} using energy-dispersive X-ray spectroscopy.[43]

PMG-CNT-CP electrodes were employed in a 20 mL NADH oxidation reactor initially containing 0.94 mM NADH. Figure 3 indicates the decrease of NADH concentration with time (blue squares), showing good agreement with simulation results (dashed lines). In this batch reactor experiment, NADH is consumed by electrochemical reaction and self-decay. Since the NADH concentration (initially ~1 mM) is lower than the K_S value (7.0 ± 0.6 mM),[43] the electrochemical rate is proportional to its concentration during the bulk oxidation. Because the NADH decay rate is small, NADH consumption is dominated by conversion to NAD^+, and an exponential decrease in concentration is observed in Figure 3. The rate of NADH consumption appears to depend linearly on the NADH concentration for the entire reaction, and the reaction solution remained homogeneous. From these observations, we may conclude that the products of NADH oxidation do not deactivate the electrode and may be mostly soluble.

About 80% conversion of NADH was observed after 1 h, suggesting a high conversion rate. As described by eq 2, NADH may be consumed by either electrooxidation or by self-decay. After 150 min of reaction, according to eq 6, 0.87 mM NAD^+ was expected to be generated, accounting for 93% of the initial NADH concentration. Over the same period, 5% of the initial NADH was predicted to be lost to self-decay, according to eq 5. This indicated that the electrochemical conversion rate was at least 13-fold higher than the decay rate.

Bioactivity of Electrogenerated NAD^+. Using the commercially available enzyme cycling assay, the yield of enzymatically active NAD^+ electrogenerated by NADH oxidation was obtained during and after electrocatalysis. The dashed lines in Figure 4 represent 100% yield of active NAD^+. During NADH electrocatalysis on the PMG-CNT modified electrode, the yield of the active NAD^+ stays at a high level. At the end of the reaction, 93 ± 6% and 87 ± 8% yields were obtained for applied potentials at 500 and 150 mV vs Ag|AgCl, respectively. This suggests that, after accounting for self-decay using eq 5, roughly 10% of the oxidized NADH may be inactive because of dimerization or some other side byproduct.

CONCLUSION

Electropolymerizing methylene green on a carboxylated-CNT-modified carbon paper yields a high-surface-area electrode with high oxidative conversion of NADH to bioactive NAD^+. Experimental data in an NADH electro-oxidizing batch reactor shows good agreement with a quantitative mathematical model. These findings demonstrate that a high-surface area poly-(azine)-CNT electrode presents a promising approach to regenerating NAD^+ for bioconversion, bioenergy, and biosensors.

ASSOCIATED CONTENT

Supporting Information

Details of the experimental measurement of NADH self-decay, model details, and parameters. This information is available free of charge via the Internet at http://pubs.acs.org/.

AUTHOR INFORMATION

Corresponding Author

*E-mail: scb@msu.edu.

Notes

The authors declare no competing financial interest.

ACKNOWLEDGMENTS

The authors gratefully acknowledge financial support from the National Science Foundation (Award CBET-0756703).

REFERENCES

(1) *CRC Handbook of Chemistry and Physics*, 91st ed.; Haynes, W. M., Ed.; CRC Press: Boca Raton, 2010.
(2) Karyakin, A. A.; Karyakina, E. E.; Schuhmann, W.; Schmidt, H. L. *Electroanalysis* **1999**, *11*, 553.
(3) Zhao, X. Ph.D. thesis, University of Minnesota, 2010.
(4) Manjon, A.; Obon, J. M.; Casanova, P.; Fernandez, V. M.; Ilborra, J. L. *Biotechnol. Lett.* **2002**, *24*, 1227.
(5) Kohlmann, C.; Markle, W.; Lutz, S. *J. Mol. Catal. B: Enzym.* **2008**, *51*, 57.
(6) Halliwell, C. M.; Simon, E.; Toh, C. S.; Bartlett, P. N.; Cass, A. E. G. *Anal. Chim. Acta* **2002**, *453*, 191.
(7) Zhang, M.; Mullens, C.; Gorski, W. *Anal. Chem.* **2007**, *79*, 2446.
(8) Ikeda, T.; Kano, K. *J. Biosci. Bioeng.* **2001**, *92*, 9.
(9) Palmore, G. T. R.; Bertschy, H.; Bergens, S. H.; Whitesides, G. M. *J. Electroanal. Chem.* **1998**, *443*, 155.
(10) Alpat, S.; Telefoncu, A. *Sensors* **2010**, *10*, 748.
(11) Akers, N. L.; Moore, C. M.; Minteer, S. D. *Electrochim. Acta* **2005**, *50*, 2521.
(12) Rincon, R. A. Ph.D. thesis, The University of New Mexico, 2010.
(13) Kinoshita, H.; Torimura, M.; Yamamoto, K.; Kano, K.; Ikeda, T. *J. Electroanal. Chem.* **1999**, *478*, 33.
(14) Togo, M.; Takamura, A.; Asai, T.; Kaji, H.; Nishizawa, M. *Electrochim. Acta* **2007**, *52*, 4669.
(15) Barton, S. C.; Gallaway, J.; Atanassov, P. *Chem. Rev.* **2004**, *104*, 4867.

(16) Gorton, L.; Dominguez, E. *J. Biotechnol.* **2002**, *82*, 371.
(17) Dilgin, Y.; Gorton, L.; Nisli, G. *Electroanalysis* **2007**, *19*, 286.
(18) Rincón, R.; Artyushkova, K.; Mojica, M.; Germain, M.; Minteer, S.; Atanassov, P. *Electroanalysis* **2010**, *22*, 799.
(19) Bartlett, P. N.; Birkin, P. R.; Wallace, E. N. K. *J. Chem. Soc., Faraday Trans.* **1997**, *93*, 1951.
(20) Kim, Y. H.; Yoo, Y. J. *Enzyme Microb. Technol.* **2009**, *44*, 129.
(21) Kim, Y. H.; Kim, T.; Ryu, J. H.; Yoo, Y. J. *Biosens. Bioelectron.* **2010**, *25*, 1160.
(22) Bonnefoy, J.; Moiroux, J.; Laval, J.-M.; Bourdillon, C. *J. Chem. Soc., Faraday Trans. 1* **1988**, *84*, 941.
(23) Laval, J. M.; Bourdillon, C.; Moiroux, J. *J. Am. Chem. Soc.* **1984**, *106*, 4701.
(24) Laval, J. M.; Bourdillon, C.; Moiroux, J. *Biotechnol. Bioeng.* **1987**, *30*, 157.
(25) Fassouane, A.; Laval, J. M.; Moiroux, J.; Bourdillon, C. *Biotechnol. Bioeng.* **1990**, *35*, 935.
(26) Musameh, M.; Wang, J.; Merkoci, A.; Lin, Y. *Electrochem. Commun.* **2002**, *4*, 743.
(27) Wang, J. *Electroanalysis* **2005**, *17*, 7.
(28) Wildgoose, G. G.; Banks, C. E.; Leventis, H. C.; Compton, R. G. *Microchim. Acta* **2006**, *152*, 187.
(29) Xu, Z.; Gao, N.; Dong, S. J. *Talanta* **2006**, *68*, 753.
(30) Zhao, X.; Lu, X.; Tze, W. T. Y.; Wang, P. *Biosens. Bioelectron.* **2010**, *25*, 2343.
(31) Narváez Villarrubia, C. W.; Rincón, R. A.; Radhakrishnan, V. K.; Davis, V.; Atanassov, P. *ACS Appl. Mater. Interfaces* **2011**, *3*, 2402.
(32) Kumar, S. P.; Manjunatha, R.; Nethravathi, C.; Suresh, G. S.; Rajamathi, M.; Venkatesha, T. V. *Electroanalysis* **2011**, *23*, 842.
(33) Tse, D. C.-S.; Kuwana, T. *Anal. Chem.* **1978**, *50*, 1315.
(34) Zhang, L.; Li, Y.; Li, D. W.; Karpuzov, D.; Long, Y. T. *Int. J. Electrochem. Sci.* **2011**, *6*, 819.
(35) Karyakin, A. A. In *Electropolymerization: Concepts, Materials and Applications*; Wiley-VCH Verlag GmbH & Co. KGaA: Weinheim, 2010, p 93.
(36) Addo, P.; Arechederra, R.; Minteer, S. *Electroanalysis* **2010**, *22*, 807.
(37) Kelly, R. M.; Kirwan, D. J. *Biotechnol. Bioeng.* **1977**, *19*, 1215.
(38) Elving, P. J.; Schmakel, C. O.; Santhanam, K. S. V.; Zuman, P. *Crit. Rev. Anal. Chem.* **1976**, *6*, 1.
(39) Jensen, M. A.; Elving, P. J. *Biochim. Biophys. Acta* **1984**, *764*, 310.
(40) Dong-mei, Z.; Hui-Qun, F.; Hong-yuan, C.; Huang-xian, J.; Yun, W. *Anal. Chim. Acta* **1996**, *329*, 41.
(41) Gorton, L.; Bartlett, P. N. In *Bioelectrochemistry*; John Wiley & Sons, Ltd: New York, 2008, p 157.
(42) Karyakin, A. A.; Bobrova, O. A.; Karyakina, E. E. *J. Electroanal. Chem.* **1995**, *399*, 179.
(43) Li, H.; Wen, H.; Calabrese Barton, S. *Electroanalysis* **2012**, *24*, 398.
(44) Kar, P.; Wen, H.; Li, H.; Minteer, S. D.; Barton, S. C. *J. Electrochem. Soc.* **2011**, *158*, B580.
(45) Wen, H.; Nallathambi, V.; Chakraborty, D.; Calabrese Barton, S. *Microchim. Acta*, 1.
(46) *Carbon: Electrochemical and Physicochemical Properties*; 1st ed.; Kinoshita, K., Ed.; Wiley-Interscience: New York, 1988.
(47) Gibon, Y.; Larher, F. *Anal. Biochem.* **1997**, *251*, 153.
(48) Matsumura, H.; Miyachi, S. *Methods Enzymol.* **1980**, *69*, 465.
(49) Vilcheze, C.; Weisbrod, T. R.; Chen, B.; Kremer, L.; Hazbon, M. H.; Wang, F.; Alland, D.; Sacchettini, J. C.; Jacobs, W. R. *Antimicrob. Agents Chemother.* **2005**, *49*, 708.
(50) Greenbau., Al; Clark, J. B.; Cmlean, P. *Biochem. J.* **1965**, *95*, 161.
(51) Lowry, O. H.; Rock, M. K.; Schulz, D. W.; Passonneau, J. V. *J. Biol. Chem.* **1961**, *236*, 2746.
(52) Biellmann, J. F.; Lapinte, C.; Haid, E.; Weimann, G. *Biochemistry* **1979**, *18*, 1212.
(53) Lowry, O. H.; Rock, M. K.; Passonneau, J. V. *J. Biol. Chem.* **1961**, *236*, 2756.
(54) Hofmann, D.; Wirtz, A.; Santiago-Schubel, B.; Disko, U.; Pohl, M. *Anal. Bioanal. Chem.* **2010**, *398*, 2803.
(55) Lowry, O. H.; Passonneau, J. V.; Schulz, D. W.; Rock, M. K. *J. Biol. Chem.* **1961**, *236*, 2746.